

Activation of Alkenes and H₂ by [Fe]-H₂ase Model Complexes

Xuan Zhao, Chao-Yi Chiang, Matthew L. Miller, Marilyn V. Rampersad, and Marcetta Y. Darensbourg*

Contribution from the Department of Chemistry, Texas A&M University, College Station, Texas 77843

Received August 5, 2002; E-mail: marcetta@mail.chem.tamu.edu

Abstract: The established ability of the Fe(II) bridging hydride species $(\mu\text{-H})(\mu\text{-pdt})[\text{Fe}(\text{CO})_2(\text{PMe}_3)]_2^+$, **1-H**⁺, to take-up and heterolytically activate dihydrogen, resulting in H/D scrambling of H₂/D₂ and H₂/D₂O mixtures (Zhao et al. *Inorg. Chem.* **2002**, *41*, 3917) has prompted a study of simultaneous alkene/H₂ activation by such [Fe]H₂ase model complexes. That the required photolysis produced an open site was substantiated by substitution of CO in **1-H**⁺ by CH₃CN with formation of structurally characterized $\{(\mu\text{-H})(\mu\text{-pdt})[\text{Fe}(\text{CO})_2(\text{PMe}_3)]_2^+\}[\text{PF}_6]^-$. Under similar photolytic conditions, H/D exchange reactions between D₂ and terminal alkenes (ethylene, propene and 1-butene), but not bulkier alkenes such as 2-butene or cyclohexene, were catalyzed by **1-H**⁺ and the edt (SCH₂CH₂S) analogue, **2-H**⁺. Substantial regioselectivity for H/D exchange at the internal vinylic hydrogen was observed. The extent to which the olefins were deuterium enriched vs deuterated was catalyst dependent. The stabilizing effect of the binuclear chelating ligands, SCH₂CH₂CH₂S, pdt, and SCH₂CH₂S, edt, is required for the activity of binuclear catalysts, as the mono-dentate $\mu\text{-SEt}$ analogue decomposed to inactive products under the photolytic conditions of the catalysis. Reactions of **1** and **2** with EtOSO₂CF₃ yielded the S-alkylated products, $\{(\mu\text{-SCH}_2\text{CH}_2\text{CH}_2\text{SEt})[\text{Fe}(\text{CO})_2(\text{PMe}_3)]_2^+\}[\text{SO}_3\text{CF}_3]^-$ (**1-Et**⁺), and **2-Et**⁺, rather than $\mu\text{-C}_2\text{H}_5$ analogues to the $\mu\text{-H}$ of **1-H**⁺. The stability and lack of reactivity toward H₂ of **1-Et**⁺ and **2-Et**⁺, indicates they are not on the reaction path of the olefin/D₂ H/D exchange process. A mechanism with olefin binding to an open site created by CO loss and formation of an Fe-(CH₂CHDR) intermediate is indicated. A likely role of a binuclear chelate effect is implicated for the unique S-XXX-S cofactor in the active site of [Fe]H₂ase.

Introduction

With the exception of vitamin B₁₂ chemistry, few organometallic processes have been definitively established in nature. There is mounting evidence that metal hydrides derived from heterolytic H₂ splitting are important intermediates along the reaction path of H₂-producing and H₂-uptake enzymes, i.e., the hydrogenases.¹⁻⁴ In particular, the H-cluster (Hydrogen-producing cluster) of Fe-only hydrogenase contains a dinuclear iron unit that is well modeled by easily prepared and classical organometallic complexes, $(\mu\text{-SRS})[\text{Fe}(\text{CO})_2\text{L}]_2$.⁵⁻¹⁰ With L = CN and R = -(CH₂)₃-, or -(CH₂NMeCH₂)- the closest

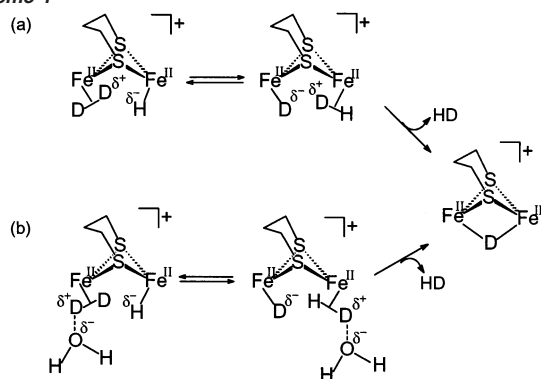
compositional analogues are obtained. Because PMe₃ imparts similar electronic characteristics to Fe as does CN⁻, without the complications of cyanide nitrogen reactivity (H-bonding protects this nitrogen when the unit is buried in the protein), the protonated form of $(\mu\text{-pdt})[\text{Fe}(\text{CO})_2(\text{PMe}_3)]_2$ complex **1**, was recently prepared, characterized as a bridging hydride $(\mu\text{-H})(\mu\text{-pdt})[\text{Fe}(\text{CO})_2(\text{PMe}_3)]_2^+[\text{PF}_6]^-$, **1-H**⁺, and explored as a functional mimic of the enzyme.^{11,12} For example, mixtures of H₂ and D₂ are converted into statistical quantities of H₂/HD/D₂ in the presence of catalytic amounts of **1-H**⁺ and under photolysis. With D₂O as deuterium source, the conversion of **1-H**⁺ into **1-D**⁺ is slower, however in the presence of D₂ and light, the bridging hydride readily becomes a bridging deuteride (within hours under sunlight).^{11,12} Both processes are impeded by added CO, similarly to the CO-inhibited enzyme.¹³

We have proposed that the above results are consistent with a mechanism that calls upon a hydride shift to change the bridging hydride of **1-H**⁺ into a terminal hydride. The opened coordination site permits $\eta^2\text{-H}_2$ binding to Fe^{II}, an interaction with much precedent.^{14,15} Alternatively, the open site requirement may be met by loss of a CO ligand, followed by D₂ capture

- (1) Krasna, A. I.; Rittenberg, D. *J. Am. Chem. Soc.* **1954**, *76*, 3015.
- (2) van der Zwaan, J. W.; Albracht, S. P. J.; Fontijn, R. D.; Slater, E. C. *FEBS Lett.* **1985**, *179*, 271.
- (3) Roberts, L. M.; Lindahl, P. A. *Biochemistry* **1994**, *33*, 14 339.
- (4) Sellmann, D.; Gottschalk-Gaudig, T.; Heinemann, F. *Inorg. Chem.* **1998**, *37*, 3982.
- (5) Peters, J. W.; Lanzilotta, W. N.; Lemon, B. J.; Seefeldt, L. C. *Science*, **1998**, *282*, 1853.
- (6) Nicolet, Y.; Piras, C.; Legrand, P.; Hatchikian, C. E.; Fontecilla-Camps, J. C. *Structure* **1999**, *7*, 13.
- (7) Nikolett, Y.; De Lacey, A. L.; Vernède, X.; Fernandez, V. M.; Hatchikian, E. C.; Fontecilla-Camps, J. C. *J. Am. Chem. Soc.* **2001**, *123*, 1596.
- (8) (a) Schmidt, M.; Contakes, S. M.; Rauchfuss, T. B. *J. Am. Chem. Soc.* **1999**, *121*, 9736. (b) Lawrence, J. D.; Li, H.; Rauchfuss, T. B.; Benard, M.; Rohmer, M.-M. *Angew. Chem., Int. Ed.* **2001**, *40*, 1768. (c) Li, H.; Rauchfuss, T. B. *J. Am. Chem. Soc.* **2002**, *124*, 726.
- (9) Lyon, E. J.; Georgakaki, I. P.; Joseph H. Reibenspies, J. H.; Darensbourg, M. Y. *Angew. Chem., Int. Ed. Engl.* **1999**, *38*, 3178.
- (10) (a) Cloirec, A. Le; Davies, S. C.; Evans, D. J.; Hughes, D. L.; Pickett, C. J.; Best, S. P.; Borg, S. *Chem. Commun.* **1999**, *22*, 2285. (b) Razavet, M.; Davies, S. C.; Hughes, D. L.; Pickett, C. J. *Chem. Commun.* **2001**, *9*, 847.

- (11) Zhao, X.; Georgakaki, I. P.; Miller, M. L.; Mejia-Rodriguez, R.; Chiang, C.-Y.; Darensbourg, M. Y. *Inorg. Chem.* **2002**, *41*, 3917.
- (12) Zhao, X.; Georgakaki, I. P.; Miller, M. L.; Yarbrough, J. C.; Darensbourg, M. Y. *J. Am. Chem. Soc.* **2001**, *123*, 9710.
- (13) Bennett, B.; Lemon, B. J.; Peters, J. W. *Biochemistry* **2000**, *39*, 7455.

Scheme 1



and bridge-H → terminal-H shift. [Our white-light irradiation protocol permits both routes to an open site.] Heterolytic cleavage thus follows from the action of an internal base, Fe-H, on the adjacent (η²-H₂)Fe^{II} or (η²-D₂)Fe^{II}, Scheme 1 (a). Alternatively, the external base H₂O may deprotonate the (η²-D₂)Fe^{II}, ultimately leaving behind an Fe-D for the reformation of the bridging deuteride, effecting H/D exchange into the catalyst as well as into the substrates, Scheme 1 (b). This working hypothesis provides an attractive basis for the existence of close-coupled binuclear active sites which utilize base metals in natural organometallic catalysts, and which perform processes reserved for expensive noble metal catalysts in the chemical industry.

The ability of a complex to activate dihydrogen has, in the history of organometallic chemistry, served as a harbinger for other bond activation processes. Two preeminent systems appropriate to our discussion are (1) the heterolytic activation of H₂ by nonredox active Ag⁺, in the presence of acetate or amine bases (preceded no doubt by a transient (η²-H₂)Ag⁺ complex);¹⁶ and (2) the homolytic activation of H₂ by Vaska's Ir^I complex, resulting in the stable Ir^{III}(H)₂ complex.¹⁷ Both of these demonstrated sluggish H/D exchange activity; neither was promising as olefin hydrogenation catalysts. Their importance lies in the precedents they set for mechanistic insight and catalyst development, which has been truly great.

As the proposed binuclear intermediates or transition states depicted in Scheme 1 are based on the hypothesis of a binuclear assembly of substrates, we have exposed the **1-H**⁺ complexes and analogues to olefins in the presence of D₂ under the conditions that effected H/D exchange in H₂/D₂ mixtures. This manuscript describes those results.

Experimental Section

Materials and Techniques. All manipulations were performed using standard Schlenk-line and syringe/rubber septa techniques under N₂ or in an argon atmosphere glovebox. Dichloromethane was distilled over P₂O₅ under N₂. Compounds (μ-pdt)[Fe(CO)₂(PMe₃)₂], **1**; (μ-edt)[Fe(CO)₂(PMe₃)₂], **2**; {(μ-H)(μ-pdt)[Fe(CO)₂(PMe₃)₂]⁺[PF₆]⁻, **1-H**⁺; and {(μ-H)(μ-edt)[Fe(CO)₂(PMe₃)₂]⁺[PF₆]⁻, **2-H**⁺, were synthesized as reported.^{11,12} The following materials were of reagent grade and used

as received (Aldrich Chemical Co.): Fe₃(CO)₁₂, 1,3-propanedithiol, 1,2-ethanedithiol, C₂H₅OSO₂CF₃, ¹³CH₃OSO₂CF₃ (98 atom % ¹³C), concentrated HCl and NH₄PF₆, ethylene, propylene, 1-butene, and C₂D₄; CD₂Cl₂ and D₂ (Cambridge Isotope Laboratories).

Infrared spectra were recorded on a Mattson Galaxy 6021 using 0.1 mm NaCl cells. ¹H, ¹³C, and ³¹P NMR (85% H₃PO₄ was used as external reference) spectra were recorded on a Unity + 300 MHz superconducting NMR instrument, operating at 299.9, 75.43, and 121.43 MHz, respectively. ²H NMR spectra were recorded on a Unity Inova-400 with a 5 mm autoswitchable probe operating at 61.35 MHz. Elemental analyses were performed by Canadian Microanalytical Services, Ltd.; Delta, British Columbia.

The X-ray crystal structures were solved at the Crystal & Molecular Structure Laboratory Center at Texas A&M University. X-ray data were collected on a Bruker Smart 1000 CCD diffractometer and covered a hemisphere of reciprocal space by a combination of three sets of exposures. Space groups were determined on the basis of systematic absences and intensity statistics. Structures were solved by direct methods. Anisotropic displacement parameters were determined for all non-hydrogen atoms. Hydrogen atoms were placed at idealized positions and refined with fixed isotropic displacement parameters. Programs used for data collection and cell refinement, SMART;¹⁸ data reduction, SAINTPLUS;¹⁹ structure solution, SHELXS-86 (Sheldrick);²⁰ structure refinement, SHELXL-97 (Sheldrick);²¹ and molecular graphics and preparation of material for publication, SHELXTL-Plus, version 5.1 or later (Bruker).²²

H/D Exchange Reactions of Alkenes/D₂. Typically, a CH₂Cl₂ solution of the hydride (**1-H**⁺ or **2-H**⁺) (ca. 20 mg, 0.032 mmol, in 0.8 mL CH₂Cl₂) was transferred to a medium-pressure NMR tube (Wilmad, 528-PV-7) in an Ar-filled glovebox. The tubes were first pressurized with alkene (ethylene, propene or 1-butene) to 2 bar, and then with D₂ to 10 bar. In side-by-side runs with a reference reaction as control, tubes were irradiated by exposure to sunlight by placing on the window sill inside a heavy Pyrex flask. The H/D exchange process was monitored by ²H NMR spectroscopy. At least four repetitions of reactions were carried out with reproducibility of relative exchange abilities on the order of ± 10%.

Reaction of {(μ-H)(μ-pdt)[Fe(CO)₂(PMe₃)₂]⁺[PF₆]⁻ with CH₃CN. To a 20 mL CH₂Cl₂ solution containing 0.250 g (0.40 mmol) **1-H**⁺ was added 1 equiv of CH₃CN via syringe. On exposure to sunlight for 4–6 h, the red orange solution color gradually changed to red brown. On completion of the reaction as indicated by disappearance of IR bands of **1-H**⁺, the solution was filtered through Celite under Ar, and the solvent was removed in vacuo to yield a dark brown gummy solid. After an ether wash, a brown solid was isolated, 0.150 g, Yield, 40%. IR (CH₂Cl₂, cm⁻¹) ν(CO): 2028 (s), 1974 (s, b). Elemental Anal. Calcd (found) for C₁₄H₂₈NO₃P₃S₂F₆Fe₂: C, 26.19 (26.28); H, 4.36 (4.38); N, 2.18 (2.16).

X-ray Diffraction Study of {(μ-H)(μ-pdt)[Fe(CO)₂(PMe₃)][Fe(CO)(CH₃CN)(PMe₃)]⁺[PF₆]⁻. Red brown crystals of {(μ-H)(μ-pdt)[Fe(CO)₂(PMe₃)][Fe(CO)(CH₃CN)–(PMe₃)]⁺[PF₆]⁻ were obtained from ether vapor diffusion into a CH₂Cl₂ solution of the salt at room temperature. *d* = 1.683 mg/m³; monoclinic P2(1)/c; unit cell dimension: *a* 17.516(4) Å, *b* 28.565(6) Å, *c* 10.116(2) Å; β 90.112(4)°; *V* 5061.8 Å³, *Z* = 8; absorption coefficient: 1.561 mm⁻¹; Reflections collected, 31 847; Wavelength, 0.710 73 Å; Final *R* indices [*I* > 2σ(*I*)], *R*₁ = 0.0743, *wR*₂ = 0.1782; *R* indices (all data), *R*₁ = 0.2285, *wR*₂ = 0.2816. A full report is available in Supporting Information.

Reaction of {(μ-H)(μ-pdt)[Fe(CO)₂(PMe₃)₂]⁺[PF₆]⁻ with C₂H₄. A solution of **1-H**⁺ (0.250 g, 0.40 mmol) in 20 mL CH₂Cl₂ (100 mL

(14) Rocchini, E.; Rigo P.; Mezzetti, A.; Stephan, T.; Morris R. H.; Lough, A. J.; Forde, C. E.; Fong, T. P.; Drouin S. D. *J. Chem. Soc., Dalton Trans.* **2000**, 20, 3591.

(15) (a) Kubas, G. J. *Acc. Chem. Res.* **1988**, *21*, 120–128. (b) Kubas, G. J. *Metal Dihydrogen and σ-Bond Complexes*; Kluwer Academic/Plenum Press: New York, 2001.

(16) Milne, J. B.; Halpern, J. *Proc. Second Intern. Congr. Catalysis, Ed. Technip, Paris*, **1961**, p 445.

(17) Eberhardt, G. G.; Vaska, L. *J. Catal.* **1967**, *8*, 183.

(18) SMART 1000 CCD, Bruker Analytical X-ray Systems; Madison, WI, 1999.

(19) SAINT-Plus, version 6.02; Bruker, Madison, WI, 1999.

(20) Sheldrick, G. SHELXS-86: Program for Crystal Structure Solution; Institut für Anorganische Chemie der Universität: Göttingen, Germany, 1986.

(21) Sheldrick, G. SHELXL-97: Program for Crystal Structure Refinement; Institut für Anorganische Chemie der Universität: Göttingen, Germany, 1997.

(22) SHELXTL, version 5.1 or later; Bruker, Madison, WI, 1998.

Pyrex Schlenk flask) was purged with C_2H_4 and irradiated by sunlight for ~ 8 h. The solution color changed from red orange to dark brown. The IR spectrum of the resulting solution showed $\nu(CO)$ bands at 2048 (w), 2025 (s) and 1982 (s) cm^{-1} .

Reaction of $EtOSO_2CF_3$ with $(\mu-SRS)[Fe(CO)_2(PMe_3)_2]$ (SRS = pdt and edt) and Characterization of $\{(\mu-SRSEt)[Fe(CO)_2(PMe_3)_2]\}^+ [SO_3CF_3]^-$ ($R = C_3H_6$, $1-Et^+$; $R = C_2H_4$, $2-Et^+$). The following procedure was used for both. A 100 mL Schlenk flask was charged with 0.460 g (0.95 mmol) $(\mu-pdt)[Fe(CO)_2(PMe_3)_2]$ and 0.360 g (2.0 mmol) $EtOSO_2CF_3$. 20 mL of CH_2Cl_2 were added to this flask and the solution was stirred at room temperature until the reaction was complete as indicated by IR (~ 8 h). The solvent was removed under vacuum and the residue was washed with 4×20 mL ether until the red orange oil solidified. Yield, 0.450 g, 70%, $1-Et^+$. IR (CH_2Cl_2 , cm^{-1}) $1-Et^+$, $\nu(CO)$: 2011 (m), 1981 (s), 1950 (s), 1939 (sh). 1H NMR (CD_2Cl_2 at 22 $^\circ C$): 1.69 (d, $J_{P-H} = 10$ Hz, 18 H, $P(CH_3)_3$), 2.86 (b, 2H, $C-CH_2-C$ of $\mu-pdt$), 2.17 (t, 4H, CH_2-S of $\mu-pdt$), 3.0 (q, 7.2 Hz, 2 H, SCH_2-CH_3), 1.52 (7.2 Hz, 3 H, SCH_2CH_3). ^{31}P NMR (CD_2Cl_2 at 22 $^\circ C$): 20.2 (s, PMe_3). Elemental Anal. Calcd. (found) for $1-Et^+$ $C_{16}H_{29}O_7P_2S_3F_3Fe_2$: C, 29.12 (28.84); H, 4.39 (4.44).

A similar yield was obtained for $2-Et^+$. IR (CH_2Cl_2 , cm^{-1}) $2-Et^+$, $\nu(CO)$: 2013 (m), 1983 (s), 1952 (s), 1942 (sh). 1H NMR (d^6 -acetone at 22 $^\circ C$): 1.71 (d, $J_{P-H} = 9.9$ Hz, 18 H, $P(CH_3)_3$), 3.38 (t, 2 H, $J = 6.6$ Hz, $CH_3CH_2S-CH_2CH_2-S$), 2.45 (t, $J = 6.6$ Hz, 2 H, $CH_3CH_2S-CH_2CH_2-S$), 3.75 (q, 7.2 Hz, 2 H, SCH_2CH_3), 1.71 (7.2 Hz, 3 H, SCH_2CH_3). ^{31}P NMR (d^6 -acetone at 22 $^\circ C$): 19.6 (s, PMe_3).

X-ray Crystal Structure Analysis of $2-Et^+$. Red orange crystals of $2-Et^+$ were obtained from layering of ether over a CH_2Cl_2 solution of $2-Et^+$ at -5 $^\circ C$. $d = 1.574$ mg/m^3 ; triclinic P-1; unit cell dimension: a 11.046(2) \AA , b 16.325(4) \AA , c 16.485(4) \AA ; α 117.955(4) $^\circ$, β 97.071(4) $^\circ$, γ 91.898(4) $^\circ$; V 2591.6(10) \AA^3 , $Z = 4$; absorption coefficient: 1.456 mm^{-1} ; Reflections collected, 11 608; Wavelength, 0.710 73 \AA ; Final R indices [$I > 2\sigma(I)$], $R_1 = 0.0747$, $wR_2 = 0.1768$; R indices (all data), $R_1 = 0.0967$, $wR_2 = 0.2013$.

Reaction of $^{13}CH_3OSO_2CF_3$ with $(\mu-pdt)[Fe(CO)_2(PMe_3)_2]$. In a manner similar to that described above, 0.700 g **1** and 1.00 g $^{13}CH_3OSO_2CF_3$ were mixed, ultimately yielding 0.750 g (80%) of a red orange solid, $1-^{13}CH_3^+$. IR (CH_2Cl_2 , cm^{-1}) $1-^{13}CH_3^+$, $\nu(CO)$: 2013 (m), 1983 (s), 1951 (s), 1940 (sh). 1H NMR (CD_2Cl_2 at 22 $^\circ C$): 1.69 (d, $J_{P-H} = 9.6$ Hz, 18 H, $P(CH_3)_3$), 2.86 (b, 2H, $C-CH_2-C$ of $\mu-pdt$), 2.16 (b, 4H, CH_2-S of $\mu-pdt$), 2.81 (d, 144 Hz, 3 H, SCH_3). ^{31}P NMR (d^6 -acetone at 22 $^\circ C$): 21.4 (s, PMe_3). ^{13}C NMR (CD_2Cl_2 at 22 $^\circ C$): 33.0 (s, $^{13}CH_3$).

Results and Discussion

H/D Exchange between C_2D_4 and $\{(\mu-H)(\mu-SRS)[Fe(CO)_2(PMe_3)_2]\}^+ [PF_6]^-$. The experimental protocol used to establish H/D exchange catalysis in H_2/D_2 mixtures was used here.^{11,12} Solutions of $\{(\mu-H)(\mu-SRS)[Fe(CO)_2(PMe_3)_2]\}^+ [PF_6]^-$ (SRS = pdt, $1-H^+$, and edt, $2-H^+$) in CH_2Cl_2 were placed in medium-pressure NMR tubes which were evacuated and backfilled with C_2D_4 to 1 bar. No changes were observed when stored for > 12 h in the dark, however on exposure to natural sunlight for even short periods of time (1–2 h), triplets characteristic of the $(\mu-D)Fe^{II}_2$ species appeared in the high field region of the 2H NMR spectra. When a mixture of both hydrides, $1-H^+$, and $2-H^+$, in identical concentrations, and C_2D_4 (1 bar) was exposed to sunlight for 2 h, the greater intensity of the $\{(\mu-D)(\mu-edt)[Fe(CO)_2(PMe_3)_2]\}^+ [PF_6]^-$, $2-D^+$, resonance at -17.44 ppm indicated a faster rate of exchange for the 2-carbon bridged species, Figure 1. Such single tube competition experiments, or side-by-side experiments, permitted comparisons of reactivity under identical conditions.

H/D Exchange between C_2H_4 and D_2 . The abilities of compounds $1-H^+$ and $2-H^+$ to catalyze reactions of C_2H_4 and

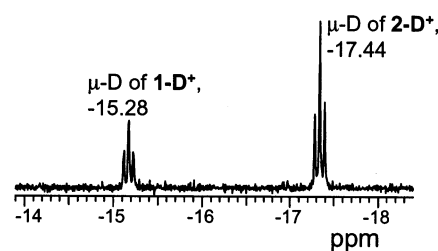


Figure 1. High field 2H NMR spectrum ($\mu-H$ region) showing deuteration-enrichment in a 1:1 mixture of $\{(\mu-H)(\mu-pdt)[Fe(CO)_2(PMe_3)_2]\}^+ [PF_6]^-$ and $\{(\mu-H)(\mu-edt)[Fe(CO)_2(PMe_3)_2]\}^+ [PF_6]^-$ in CH_2Cl_2 pressurized with C_2D_4 to 1 bar following exposure to sunlight for 2 h.

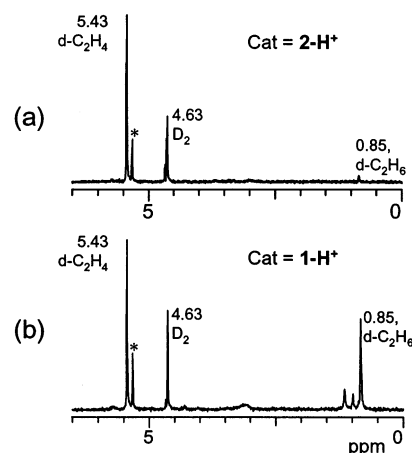


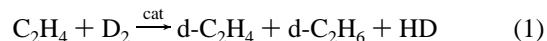
Figure 2. Low field 2H NMR spectrum showing H/D exchange between C_2H_4 (2 bar) and D_2 (8 bar) in CH_2Cl_2 in the presence of (a) $\{(\mu-H)(\mu-edt)[Fe(CO)_2(PMe_3)_2]\}^+ [PF_6]^-$; (b) $\{(\mu-H)(\mu-pdt)[Fe(CO)_2(PMe_3)_2]\}^+ [PF_6]^-$ following exposure to sunlight for 5 h. *Natural abundance of D in CH_2Cl_2 solvent, 5.32 ppm.

Table 1. D-incorporation/Exchange into C_2H_4 and Deuterated C_2H_6 Measured by NMR Peak Intensities Relative to Solvent

catalyst	time (h) ^a	d- C_2H_4	d- C_2H_6	total D
$\{(\mu-H)(\mu-pdt)[Fe(CO)_2(PMe_3)_2]\}^+$	5	4.4	1.8	6.2
	30	5.0	4.1	9.1
$\{(\mu-H)(\mu-edt)[Fe(CO)_2(PMe_3)_2]\}^+$	5	6.9	0.1	7.0
	30	14.0	0.81	14.8

^a Recorded as hours of sunlight irradiation.

D_2 , eq 1, were compared in side-by-side NMR tube reaction



studies using 2H NMR spectroscopy as monitor of D-enrichment. Solutions of the catalysts were pressurized with C_2H_4 (2 bar), and further with D_2 (8 bar), and then exposed to sunlight. The formation of HD could be discerned as a shoulder (4.67 ppm) on the resonance for dissolved D_2 (4.63 ppm); an intense resonance at 5.43 ppm indicated 2H -enriched ethylene. Using the resonance for natural abundance deuterium in the CH_2Cl_2 as an internal standard, the relative amount of 2H enrichment was measured to be 6.9 times that of the solvent after exposure to sunlight for 5 h for the $2-H^+$ catalyst. With $1-H^+$ as catalyst, the relative intensity of d- C_2H_4 to d- CH_2Cl_2 was 4.4 and 5.0 after 5- and 30-h exposure, respectively, Figure 2 and Table 1. The high field region of the spectrum showed $(\mu-D)Fe_2^+$ formation.

Also clearly seen in Figure 2a is the resonance for 2H -enriched C_2H_6 at 0.85 ppm. In contrast to the $1-H^+$ catalyzed reaction,

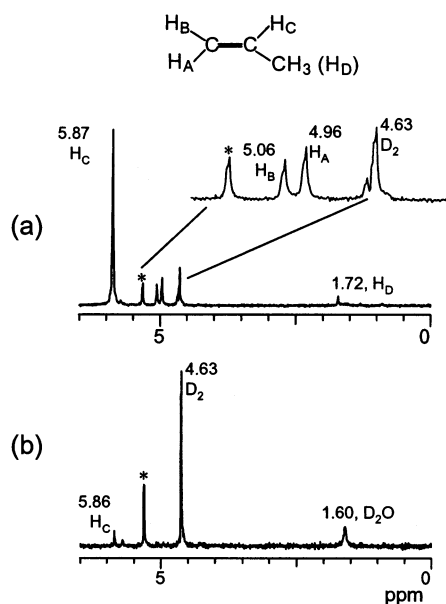


Figure 3. Low field ^2H NMR spectrum showing H/D exchange between C_3H_6 (2 bar) and D_2 (8 bar) in CH_2Cl_2 in the presence of (a) $\{(\mu\text{-H})(\mu\text{-edt})\text{Fe}(\text{CO})_2(\text{PMe}_3)_2\}^+[\text{PF}_6]^-$; b) $\{(\mu\text{-H})(\mu\text{-pdt})\text{Fe}(\text{CO})_2(\text{PMe}_3)_2\}^+[\text{PF}_6]^-$ following exposure to sunlight for 5 h.

that position shows only minor intensity for 2-H^+ as a catalyst. The reproducibility of this experimental design is high (ca. 5 repetitions with differences on the order of 10–15%) in terms of relative amounts of products both within the individual runs and between catalysts.

Compounds $\{(\mu\text{-H})(\mu\text{-SEt})\text{Fe}(\text{CO})_2(\text{PMe}_3)_2\}^+[\text{PF}_6]^-$ and $\{(\mu\text{-H})(\mu\text{-oxyldt})\text{Fe}(\text{CO})_2(\text{PMe}_3)_2\}^+[\text{PF}_6]^-$ (o-xyldt = $\text{SCH}_2\text{C}_6\text{H}_4\text{-CH}_2\text{S}$) were also checked for catalytic activity for the H/D exchange reaction between C_2H_4 and D_2 . Very small amounts of $d\text{-C}_2\text{H}_4$ were observed as these two hydrides decomposed within 2 h and insoluble solids precipitated out in the NMR tube.

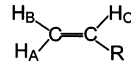
H/D Exchange between Propene and D_2 . The reaction of C_3H_6 with D_2 was catalyzed by 1-H^+ and 2-H^+ resulting in the formation of D-enriched propene and $d\text{-C}_3\text{H}_8$, similarly to the reaction between C_2H_4 and D_2 . Figure 3a shows the ^2H NMR spectrum recorded after 5 h of H/D exchange with 2-H^+ as catalyst. The resonance at 5.87 ppm, representing the internal vinyl proton, is 8.4 times the intensity of the natural abundance ^2H in the CH_2Cl_2 solvent. Resonances at 5.06 and 4.96 ppm show slight enrichment, whereas the terminal methyl group shows even less. In contrast, with 1-H^+ as a catalyst virtually no exchange is observed. Again, these experiments were repeated 4 times under side-by-side photolytic conditions with the same relative order of enrichment and reduction products. The relative intensities from a representative run are listed in Table 2.

H/D Exchange between 1-Butene and D_2 . The experimental data for H/D exchange between 1-butene and D_2 is listed in Table 2. It is again observed that the 2-H^+ catalyst promotes H/D exchange into the internal H_C position and is much more effective than the 1-H^+ analogue.

More hindered alkenes such as 2-butene, isobutene, and cyclohexene showed negligible H/D exchange with either 1-H^+ or 2-H^+ as catalysts.

Stoichiometric Reaction of $\{(\mu\text{-H})(\mu\text{-pdt})\text{Fe}(\text{CO})_2(\text{PMe}_3)_2\}^+[\text{PF}_6]^-$ with Olefins: IR Monitors. Notable shifts

Table 2. D-Incorporation/Exchange into C_nH_{2n} and Deuterated $\text{C}_n\text{H}_{2n+2}$ Measured by NMR Peak Intensities Relative to Solvent



catalyst	R	time (h)	H_A	H_B	H_C	$d\text{-C}_n\text{H}_{2n+2}$	total D
1-H^+	CH_3	5	0.09	0.07	0.26	0.22	0.64
		30	0.39	0.31	1.0	0.61	2.3
2-H^+	C_2H_5	5	0.14	0.12	0.96	0.80	2.0
		30	0.60	0.50	3.93	2.3	7.3
2-H^+	CH_3	5	0.59	0.45	4.57		6.6
		30	2.42	1.85	10.7	0.20	15.0
2-H^+	C_2H_5	5	0.13	0.15	1.82		2.1
		30	1.46	1.74	13.2		16.4

were observed in the $\nu(\text{CO})$ region of the infrared spectra taken on samples removed from NMR tubes following the H/D exchange experiments described above for D_2 and C_2H_4 . To explore the possibility that stable intermediates or products might result from substrate capture by an opened site on the catalyst, a CH_2Cl_2 solution of 1-H^+ was saturated with C_2H_4 and stirred at room temperature under ambient laboratory lighting conditions for 1 day; the solution color changed from red orange to dark brown. The $\nu(\text{CO})$ bands in the IR spectrum of the starting material at 1991 (s), 2033 (s) cm^{-1} shifted to 1982 and 2025 cm^{-1} and an additional band was seen at 2048 cm^{-1} , see Supporting Information. These are identical to $\nu(\text{CO})$ spectra removed from the pressure NMR tubes, following H/D exchange experiments with D_2 and C_2H_4 . No such shifts were observed from samples in which only D_2 or H_2 was added to the $\{(\mu\text{-H})(\mu\text{-SRS})\text{Fe}(\text{CO})_2(\text{PMe}_3)_2\}^+[\text{PF}_6]^-$ solutions. With propene and butene as substrates, the $\nu(\text{CO})$ IR spectra were unchanged over the course of the H/D exchange and hydrogenation catalysis. Thus the observed changes in the ethylene reaction are assumed to derive from CO substitution by C_2H_4 . Unfortunately we were unable to definitively characterize the product isolated from the bulk chemical reaction.

Reaction of $\{(\mu\text{-H})(\mu\text{-pdt})\text{Fe}(\text{CO})_2(\text{PMe}_3)_2\}^+$ with CH_3CN . As acetonitrile was known to inhibit the ability of 1-H^+ to promote H/D exchange reactivity in H_2/D_2 mixtures,^{11,12} the possibility that it might form a stable discrete CO substitution product was explored. Addition of one equivalent of CH_3CN to a CH_2Cl_2 solution of 1-H^+ and exposure to sunlight resulted in a gradual color change from red orange to red brown over the course of 4 to 6 h. The $\nu(\text{CO})$ bands (CH_2Cl_2 solution) shifted from 2032 (s) and 1990 (s) cm^{-1} to 2028 (s) and 1974 (s,b) cm^{-1} . Despite the simple IR spectral pattern, the ^1H NMR spectra of the reaction under similar photolytic conditions at different time intervals, vide infra, indicated the presence of two hydride-containing products. One is centered at -11.0 ppm with $J_{\text{P-H}}$ coupling constants of 21.2 and 27.6 Hz; the other hydride is at -26.2 ppm with $J_{\text{P-H}} = 22.8$ and 26.4 Hz, see Supporting Information. Thus, the hydride in both species is coupled to two different phosphine ligands, a result that was corroborated by the ^{31}P NMR spectrum. Such a high field resonance at -26 ppm is indicative of a tri- or poly-nuclear species; the one at -11 ppm, a binuclear product. The latter was confirmed by isolation and X-ray structure analysis as $\{(\mu\text{-H})(\mu\text{-pdt})\text{Fe}(\text{CO})_2(\text{PMe}_3)]\text{-}[\text{Fe}(\text{CO})(\text{CH}_3\text{CN})(\text{PMe}_3)]\}^+[\text{PF}_6]^-$, resulting from CO substitution by CH_3CN , eq 2. Interestingly, the elemental analysis for the isolated solid,

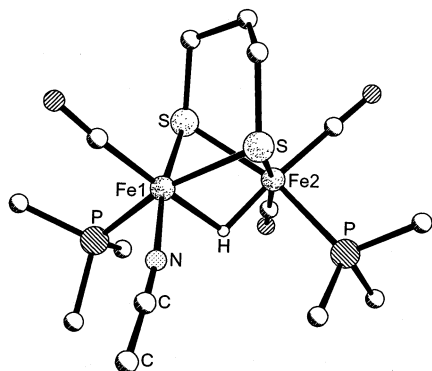
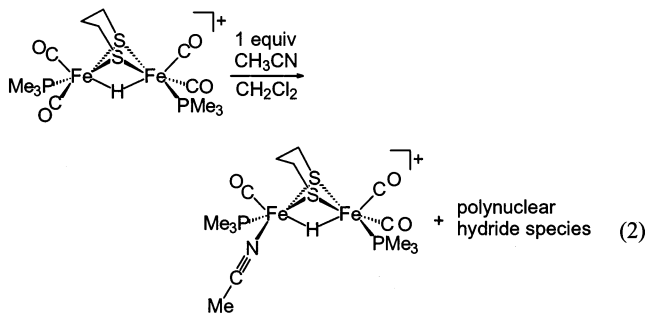


Figure 4. Ball and stick representation of the cation portion of $\{(\mu\text{-H})(\mu\text{-pdt})[\text{Fe}(\text{CO})_2(\text{PMe}_3)][\text{Fe}(\text{CO})(\text{CH}_3\text{CN})(\text{PMe}_3)]\}^+[\text{PF}_6]^-$ with the disordered methylene carbon of the propyl bridge omitted for clarity. Selected average distances (\AA): Fe1–Fe2, 2.600(2); Fe1–H, 1.8(1); Fe2–H, 1.6(1); Fe1–N, 1.95(1); Fe–P, 2.236(3); two different Fe1–S distances, 2.230(3) opposite the acetonitrile and 2.264(3) adjacent to the acetonitrile; Fe2–S, 2.281(3). Selected average bond angles ($^\circ$): Fe1–H–Fe2, 96(3); Fe–S–Fe, 70.11(9); S–Fe–S, 84.7(1); Fe–C–O, 177(1); Fe–N–C, 173.2(9); N–C–C, 178(1).

presumably a mixture of the binuclear and polynuclear species, was in precise agreement with the empirical formula of the binuclear salt. We assume therefore that the species responsible for the high field resonance is a multiple of the binuclear product, i.e., a tetranuclear species for which higher field hydride resonances might be reasonable.



The Molecular Structure of $\{(\mu\text{-H})(\mu\text{-pdt})[\text{Fe}(\text{CO})_2(\text{PMe}_3)][\text{Fe}(\text{CO})(\text{CH}_3\text{CN})(\text{PMe}_3)]\}^+[\text{PF}_6]^-$. The overall structure of this compound, Figure 4, is the same as that of the parent, $\mathbf{1-H}^+$. The iron atoms are in a distorted octahedral geometry, with an Fe–Fe distance of 2.606(2) \AA , ca. 0.02 longer than the Fe–Fe distance in $\mathbf{1-H}^+$, 2.5784(8) \AA . In both, the PMe_3 ligands are retained in the ba/ba (transoid) conformation of the neutral complex precursor and are cis to the $\text{Fe}^{\text{II}}(\mu\text{-H})\text{Fe}^{\text{II}}$ units. The substitution of a basal CO by CH_3CN on Fe(1) produces asymmetry in the binuclear cation. The bridging hydride was located upon successive recycling of the Fourier map and appears to be nearer the less electron-rich Fe(2) center (1.6(1) \AA vs 1.8(1) \AA); the level of uncertainty is however beyond 3σ .

Reactivity of $\{(\mu\text{-H})(\mu\text{-pdt})[\text{Fe}(\text{CO})_2(\text{PMe}_3)][\text{Fe}(\text{CO})(\text{CH}_3\text{CN})(\text{PMe}_3)]\}^+[\text{PF}_6]^-$. An NMR sample containing a $\text{CD}_2\text{-Cl}_2$ solution of $\mathbf{1-H}^+$, (–15.2 ppm), $\{(\mu\text{-H})(\mu\text{-pdt})[\text{Fe}(\text{CO})_2(\text{PMe}_3)][\text{Fe}(\text{CO})(\text{CH}_3\text{CN})(\text{PMe}_3)]\}^+[\text{PF}_6]^-$ (–11.0 ppm) and the unknown hydride species (–26.0 ppm) was pressurized with 5 bar CO and exposed to sunlight for 3 h. The resonance at –11.0 ppm decreased in intensity while that of the resonance at –15.2 ppm ($\mathbf{1-H}^+$) increased, thus demonstrating the reversibility of eq 2. (The resonance at –26.2 ppm was invariant). Although

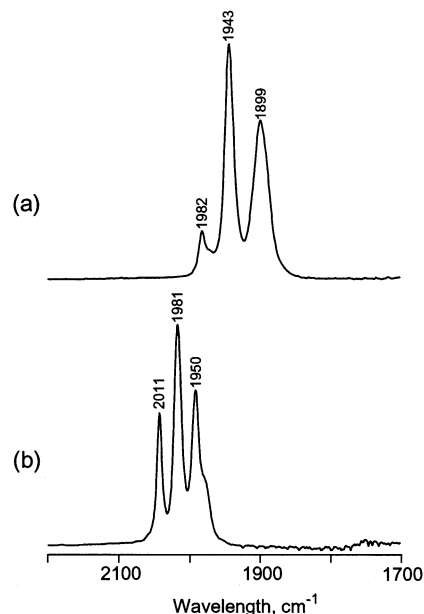


Figure 5. (a) Solution infrared spectrum of $(\mu\text{-pdt})[\text{Fe}(\text{CO})_2(\text{PMe}_3)]_2$ in CH_2Cl_2 ; (b) Solution infrared spectrum of $\mathbf{1-Et}^+$ in CH_2Cl_2 .

there is still H/D exchange between $\{(\mu\text{-H})(\mu\text{-pdt})[\text{Fe}(\text{CO})_2(\text{PMe}_3)][\text{Fe}(\text{CO})(\text{CH}_3\text{CN})(\text{PMe}_3)]\}^+[\text{PF}_6]^-$ and D_2 , resulting in the formation of $\{(\mu\text{-D})(\mu\text{-pdt})[\text{Fe}(\text{CO})_2(\text{PMe}_3)][\text{Fe}(\text{CO})(\text{CH}_3\text{CN})(\text{PMe}_3)]\}^+[\text{PF}_6]^-$ under photolytic conditions, the complex $\{(\mu\text{-H})(\mu\text{-pdt})[\text{Fe}(\text{CO})_2(\text{PMe}_3)][\text{Fe}(\text{CO})(\text{CH}_3\text{CN})(\text{PMe}_3)]\}^+[\text{PF}_6]^-$ did not take up ethylene, indicating that the acetonitrile is not to be considered as a labile ligand for purposes of substituting further with weaker donor ligands.

Synthesis of $\{(\mu\text{-SRSEt})[\text{Fe}(\text{CO})_2(\text{PMe}_3)]_2\}^+[\text{SO}_3\text{CF}_3]^-$. The possibility that an iron-bound ethyl species might be an intermediate in the catalytic $\text{C}_2\text{H}_4/\text{D}_2$ H/D exchange reaction was addressed by examining the reaction of $\text{EtOSO}_2\text{CF}_3$ as a source of Et^+ with $(\mu\text{-pdt})$ - and $(\mu\text{-edt})[\text{Fe}(\text{CO})_2(\text{PMe}_3)]_2$. Addition of three equivs of $\text{EtOSO}_2\text{CF}_3$ to a CH_2Cl_2 solution of either $\mathbf{1}$ or $\mathbf{2}$ resulted in a color change from red-brown to red-orange. The $\nu(\text{CO})$ IR spectra of the products showed four-band patterns, similar to those of the parent neutral compounds but shifted to higher energies by ca. 40 cm^{-1} , Figure 5. This shift is substantially (on average, 30 cm^{-1}) less than those of $\mathbf{1-H}^+$ or $\mathbf{2-H}^+$ (whose IR patterns are quite different from those of $\mathbf{1}$ or $\mathbf{2}$). To explore whether the Et^+ had undergone oxidative addition at the Fe–Fe bond or reacted at some other site, i.e., the sulfur of $\mu\text{-SRS}$, an isotopic labeling experiment using C-13 labeled $^{13}\text{CH}_3\text{OSO}_2\text{CF}_3$ was employed. Prepared and isolated under conditions identical to the $\text{EtOSO}_2\text{CF}_3$ reactions, the $\mathbf{1-Me}^+$ was obtained and characterized. A distinguishing feature was the lack of ^{31}P coupling to the $^{13}\text{CH}_3$ resonance (33.0 ppm) in the C-13 NMR spectrum. The conclusion of S-alkylation, Scheme 2, was corroborated by the solid-state structure of $\mathbf{2-Et}^+$. Identical results were obtained with complex $\mathbf{1}$, yielding S-alkylated $\mathbf{1-Et}^+$.

Molecular Structure of $\mathbf{2-Et}^+$. As indicated in Scheme 2 and Figure 6, the structure of the binuclear complex $\mathbf{2-Et}^+$ is largely that of the neutral precursor; the phosphine ligands remain in their same positions, ap/ba, and the coordination geometry may be viewed as edge-bridged bi-square pyramid. The Fe–Fe distance (2.567(1) \AA), however, is lengthened by

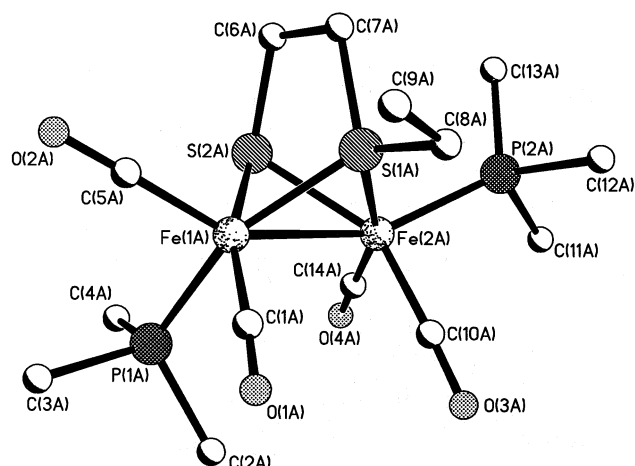
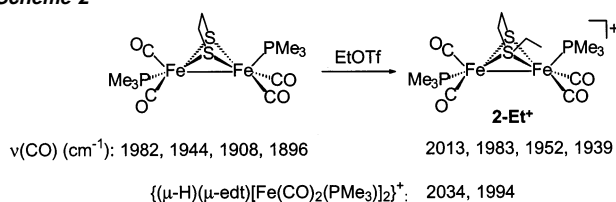


Figure 6. Ball and stick representation of the cation portion of **2-Et**⁺.

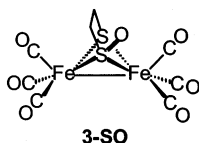
Scheme 2



ca. 0.05 Å, as compared to complex **2**. Interestingly, this distance is very close to the Fe–Fe separation in **2-H**⁺, 2.574(1) Å.¹¹

The effect of converting the bridging dithiolate into a μ -thiolate, μ -thioether is displayed in the Fe–S distances. The Fe–S_{thioether} bond distances (2.201(2) and 2.183(2) Å) are ca. 0.05 Å shorter as compared to the Fe–S_{thiolate} (2.251(2) and 2.256(2) Å) in **2-Et**⁺, to the Fe–S_{thiolate} distances in **2** (2.254(1), 2.256(1), 2.251(1) and 2.248(1) Å), and to the Fe–S_{thiolate} distances in **2-H**⁺ (2.255(2), 2.258(2), 2.253(2) and 2.259(2) Å). Similarly short Fe–S distances were observed in mono-dentate bridging thioether complexes Fe₃(CO)₈(μ -SC₄H₈)₂ and Cp*Ir(η^4 -2,5-Me₂T-Fe₂(CO)₇) (Cp* = (η^4 -C₅Me₅ and 2,5-Me₂T = 2,5-dimethylthiophene)).^{23,24}

Another example of an asymmetric bidentate chelating ligand based on edt, [μ -S(CH₂)₂S(=O)] [Fe(CO)₃]₂, complex **3-SO**, is shown in the stick drawing below.²⁴ Similarly to the **2-Et**⁺ comparison to **2**, the Fe–Fe distance of 2.528(1) Å in **3-SO** is ca. 0.04 Å longer than that of the parent, (μ -edt)[Fe(CO)₃]₂, 2.485(1) Å, and the Fe–S distance to the valence-saturated S is substantially smaller than that to the μ -thiolate: Fe–S_{sulfoxide} = 2.159(1) Å; Fe–S_{thiolate} = 2.243(1) Å.^{25,26}



Reactivity of 1-Et⁺. Compound **1-Et**⁺ is quite stable; when exposed to sunlight for 6 h, its ¹H NMR spectrum (CD₂Cl₂)

- (23) Cotton, F. A.; Troup, J. M. *J. Am. Chem. Soc.* **1974**, *96*, 5070.
 (24) Chen, J.; Daniels, L. M.; Angelici, R. J. *J. Am. Chem. Soc.* **1991**, *113*, 2544.
 (25) Messelhäuser J.; Gutensohn, K. U.; Lorenz, I.-P.; Hiller, W. *J. Organomet. Chem.* **1987**, *21*, 377.
 (26) Hughes, D. L.; Leigh, G. J.; Paulson, D. R. *Inorg. Chim. Acta* **1986**, *120*, 191.

showed no change or any insoluble decomposition products. There was no indication of the formation of the bridging hydride, **1-H**⁺, or C₂H₄, after further photolysis. On pressurizing a CH₂-Cl₂ solution of **1-Et**⁺ with D₂ (10 bar) and exposing to sunlight for ca. 10 h, there was no indication of H/D exchange reactivity or formation of $\{(\mu\text{-H/D})(\mu\text{-pdt})[\text{Fe}(\text{CO})_2(\text{PMe}_3)_2]^+\}$. Reaction with the strong acid, CF₃SO₃H, resulted in decomposition.

Comments

Several lines of evidence suggest a significant steric control of the H/D exchange in reactions of **1-D**⁺ and **2-D**⁺ with olefins. Only terminal olefins react. With propene and 1-butene, the impressive regioselectivity for H/D exchange of the vinylic proton is a result of anti-Markovnikov Fe–D addition, presumably generating an Fe–(CH₂CHD–R) intermediate. The allylic carbon shows little D incorporation, and hence olefin isomerization processes that require Fe–C_{methine} bond formation are not operative. In addition, more sterically hindered olefins do not react. Of the two stable ($\mu\text{-H})\text{Fe}_2^+$ catalysts, the one with the smaller, more restricted edt bridge is more active.

The bridging dithiolates also play a substantial role in binuclear catalyst stability, with the chelating μ -SRS more stable than two μ -SR's, demonstrating a bridging chelate effect. The bidentate, benzylic-like, o-xyldt is also unstable to the catalytic conditions, decomposing into unknown products as does the mono-dentate μ -SMe complexes. The fact that the reaction conditions that led to decomposition also showed no H/D exchange in the olefins is evidence that the intact binuclear complex is required for catalysis.

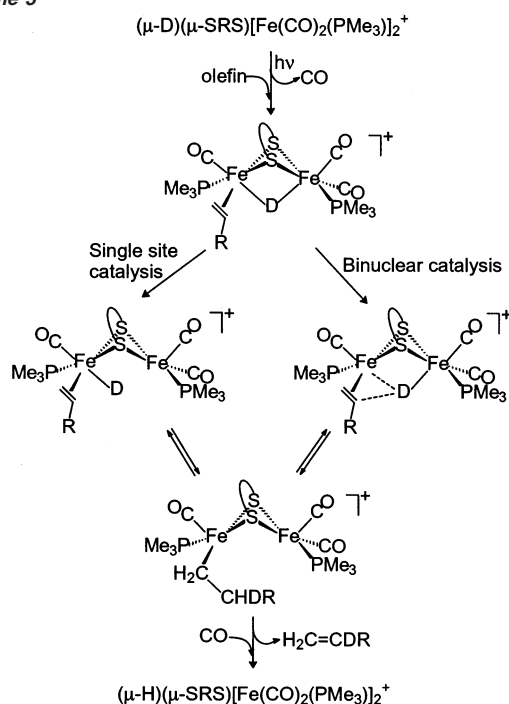
The isolation of an acetonitrile complex confirms that CO loss occurs under the same conditions as in the olefin/D₂ reaction. Its position in the basal plane is appropriate to the needed proximity of a substrate binding site to the iron-hydride. The fact that acetonitrile is replaceable only by CO, but not by ethylene, is evidence of its poor lability. Unfortunately, it does not serve as a better precursor to the catalytic open site.

The isolation of the S-alkylated, hydrocarbon-linked bridging thiolate/bridging thioether compounds **1-Et**⁺ and **2-Et**⁺ pointed to (a) the latent reactivity of the remaining lone pair on sulfur; (b) the stability of a μ -H in the binuclear iron complex over a μ -Et; and (c) the stability of a bridging thioether over a bridging thiol. Few precedents exist for μ -RSR in iron complexes.^{23,24}

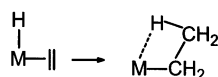
Interestingly, the change in Fe–Fe bond lengths as compared to the parent Fe^I–Fe^I complex **1**, are similar for the Fe–Fe bond-protonated, **1-H**⁺, and the S-alkylated complexes, **1-Et**⁺, products. Formation of **1-Et**⁺ and **2-Et**⁺ arguably could follow a path of Fe–Fe bond alkylation as kinetic product (the HOMO of (μ -SRS)[Fe(CO)₂(PMe₃)₂] is the Fe^I–Fe^I bond),^{11,12} with subsequent alkyl migration to the thiolate sulfur yielding the thermodynamic product. For the protonation reaction, the kinetic and thermodynamic products appear to be the same, engaging the Fe^I–Fe^I bond density. Nevertheless, the lack of reactivity of the S-alkylated complex toward D₂, under the same H/D exchange conditions that liberate CO, argues against its being an intermediate in the olefin H/D exchange process.

Whether the mechanistic paths of the olefin/ μ -HFe₂ H/D exchange process involves the binuclear collaborative effort, analogous to our previous suggestion for D₂/ μ -HFe₂ exchange, Scheme 1, is debatable. Classical organometallic olefin/M–H insertion processes which occur at a single metal center, have

Scheme 3



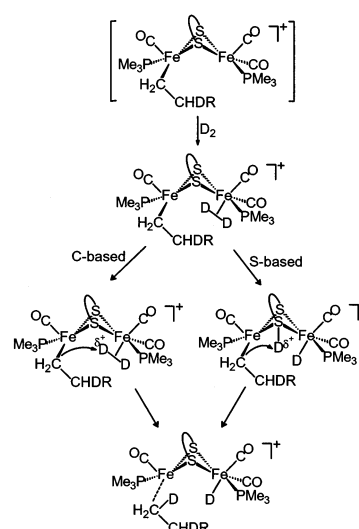
much precedent and theoretical/computational support for a transition state as shown below.²⁷



The binuclear catalyst would accommodate such an olefin/hydride insertion/ β -elimination process according to the left path of Scheme 3. The right path of Scheme 3 indicates a binuclear possibility in which the bridging hydride/terminal shift is to the iron that does not hold the olefin, permitting an internal nucleophilic attack of the hydride on the Fe-bound olefin. The binuclear path is analogous to the H_2 activation of Scheme 1, and better rationalizes the apparent steric control in the catalysis.

The saturated hydrocarbon products are rationalized according to Scheme 4. From the $\text{Fe}-\text{CH}_2\text{CHDR}$ intermediate, D_2 capture by the 16-electron Fe^{II} yields the operative $\eta^2\text{-D}_2$ intermediate. Divergent possibilities represented in Scheme 4 depict heterolytic cleavage of H_2 by the carbanion to release the DCH_2CHDR product. Alternatively, the observation of S -alkylation of the latent lone pair on the $\mu\text{-SRS}$ recalls the possibility of deuteron migration from the strong acid of $(\eta^2\text{-D}_2)\text{Fe}^{\text{II}}$ to sulfur, and hence to carbon as shown in the right side path of Scheme 4. We can confidently assume that Et^+ migration does not occur as the

Scheme 4



$\mu^2\text{-SRSEt}$ bridge ligand has been proven to be stable under catalytic conditions. Nevertheless, the possibility of migration of H^+ or D^+ to a bridging thiolato sulfur has support from computations by De Gioia et al., and Hall et al.^{28,29}

Although resolution of the mechanistic conundrums of the above will require both theory and well-designed experiments, a point to be made is the diiron catalyzed H/D exchange processes of both olefin/ D_2 and H_2/D_2 benefit from the S to S linked dithiolate as compared to the two monodentate bridges. Does this suggest one metal holds the substrate while the other provides a nucleophile for its attack, a mechanism widely ascribed to binuclear active sites in hydrolytic enzymes, and requiring minimal molecular motion? Alternatively, is the purpose of the second metal “simply” to regulate the electronic environment of the first by interacting with and modifying the ligands, generating in the case of the organometallic-like active sites of hydrogenase, for example, ligands conducive to typical insertion/deinsertion processes of soft organometallic complexes. In the above study, the reclamation of the “resting state”, the $\mu\text{-H}$ complex catalyst or precursor, again benefits from the stabilization of the bidentate bridging ligand.

Acknowledgment. We acknowledge financial support from the National Science Foundation (CHE-0111629 for this work, CHE 85-13273 for the X-ray diffractometer and crystallographic computing system) and contributions from the R. A. Welch Foundation.

Supporting Information Available: NMR and FTIR spectra as noted in text. Crystallographic (CIF) data. This material is available free of charge via the Internet at <http://pubs.acs.org>.

JA0280168

(28) Bruschi, M.; Fantucci, P.; De Gioia, L. *Inorg. Chem.* **2002**, *41*, 1421.

(29) Cao, Z.; Hall, M. B. *J. Am. Chem. Soc.* **2001**, *123*, 3734.

(27) Thorn, D. L.; Hoffmann, R. *J. Am. Chem. Soc.* **1978**, *100*, 2079.